Molecular Vision 2026; 32:472-485 <http://www.molvis.org/molvis/v32/472>
Received 4 May 2026 | Accepted 17 August 2026 | Published 30 September 2026

© 2026 Molecular Vision

Comparative RNA-Seq analysis of the extraocular muscles in mice with nystagmus.

Laura L. Johnson,[1] Juan E. Abrahante,[2] Linda K. McLoon[1]

[1]Department of Ophthalmology and Visual Neurosciences, University of Minnesota, Minneapolis, MN; [2]Minnesota Genomics Center, University of Minnesota, Minneapolis, MN

Purpose: Infantile nystagmus syndrome (INS) is a gaze-holding disorder characterized by uncontrolled eye oscillations that can result in significant loss of visual acuity. INS is often associated with albinism, but the mechanism is unclear. We tested optokinetic response (OKR) for 4 strains of albino or hypopigmented mice and control mice. RNA-Seq was performed on extraocular muscles (EOM) from the albino and hypopigmented and control mice to uncover molecular differences that may contribute to nystagmus.

Methods: OKR of all mice using an ISCAN system was performed. RNA was isolated from EOM to identify differentially expressed genes and validated with immunohistochemistry. Ingenuity pathway analyses identified top biologic pathways.

Results: All albino or hypopigmented mice tested had uncontrolled oscillatory eye movements. Differential RNA expression analysis of each albino or hypopigmented EOM sample compared to the control EOM showed 14 genes differentially expressed in every combination. Muscle specific genes, *arrdc2* and *mss51,* were chosen for further studies. Differences in gene expression were validated by immunostaining.

Conclusions: Using a combinatorial RNA-seq approach allowed the identification of genes that have not been associated with nystagmus previously, and reduced the number of potential gene targets between any two of the mouse strains with nystagmus to 14. Two of the identified genes have known roles in control of muscle structure and function that suggest they may play causative and/or compensatory role in the abnormal eye movements associated with nystagmus. While their specific roles in EOM function is unknown, these data suggest possible candidate genes related to nystagmus.

Infantile nystagmus (INS) is characterized by uncontrolled oscillatory movements of the eyes, with onset before 6 months of age [1,2], resulting in a significant loss in visual acuity in most individuals. INS is often associated with known alterations in sensory afferents to the brain, such as albinism and optic nerve hypoplasia [1]. It is also associated with several specific genetic mutations [3]. Approximately 20% of children with x-linked pedigrees of "idiopathic" INS have a mutation in the gene for *FRMD7* [4], which has been shown to control nerve outgrowth [5]. *Pax6* is a gene associated with controlling generation of specific neuronal subtypes and nerve growth [6], and mutations in this gene result in associated eye problems including aniridia [7]. Similarly, *tyr* [8], a gene associated with albinism, is associated with development of INS. The causative link between the very different effects of mutations in these genes and the resultant nystagmus is unclear. Our data showed a motor basis for the development of nystagmus in the MyoD$^{-/-}$ mouse [9,10]. Taken together, the association of quite disparate conditions associated with INS development suggests that there is a commonality between these disparate causes of INS specifically related to axon growth, pathfinding, and/or maintenance of neuromuscular junctions, resulting in insufficient signaling from the ocular motor neurons to the extraocular muscles (EOM) - and includes both sensory and motor systems. However, many individuals with INS have no known sensory afferent defects or genetic syndromes, and thus the underlying cause of their nystagmus is unknown. In light of the large number of individuals with idiopathic childhood-onset nystagmus, there is a strong rationale for attempting to discover potential causative genes that might play a role in the development and/or maintenance of INS.

We isolated RNA from the extraocular muscles from four genotypes of albino or hypopigmented mice that have nystagmus [11,12]. Specifically, we isolated RNA from these tissues in the following mouse strains: *BALB/c*, *CD-1*, *B6(Cg)-Tyr^{c-2J}/J* [B6 albino], and the hypopigmented *DBA/1J* strain and compared the collective differences with gene expression in the *C57BL/6* pigmented mouse (WT). We used RNA-Seq to identify potential gene candidates involved in either the cause or maintenance of nystagmus. In addition, these data may discover new animal models for INS, linked to previously undiscovered causative genes.

Correspondence to: Linda McLoon, Department of Ophthalmology and Visual Neurosciences University of Minnesota, Room 374 Lions Research Building, 2001 6th Street SE, Minneapolis, MN 55455; Phone: (612) 626-0777; email: mcloo001@µmn.edu

METHODS

Animals: C57BL/6, BALB/cJ, DBA1J and B6(Cg)-Tyr^{c-2J}/J (B6 albino) mice were obtained from Jackson Laboratory (Bar Harbor, ME), and *CD-1* mice were obtained from Charles River Laboratories (Wilmington, MA). They were all housed with Resource Animal Resources at the University of Minnesota with 12-h light/dark cycle and food ad libitum. All animal studies followed the guidelines of the National Institutes of Health and the Association for Research in Vision and Ophthalmology, and all experiments were approved by the Institutional Animal Care and Use Committee at the University of Minnesota (approval number 2202–39815A).

Optokinetic reflex testing (OKR): OKR was assessed as described previously [9,10,12]. In preparation for measurement of OKR, head posts were implanted to stabilize the head during testing. After making a sterile incision into the scalp, the skull was cleaned, and head-posts were implanted by first inserting 000×3/32" self-tapping screws into the mouse skull on the top of the head. Geristore dental cement (DenMat LLC, Lompoc, CA, USA) was placed on top of the screws and surrounding skull area to create a cap in which to insert the head-posts. M3×0.5mm nylon pan head slotted screws, with the screw heads removed, were placed vertically into the Geristore cement before it dried; this created posts on the mouse head for stabilization during pupil tracking experiments. Mice were allowed to recover from surgery for two weeks before testing. OKR traces were performed on a total of 6 *C57BL/6* mice, 7 *CD-1*, 4 *BALB/c*, 8 *DBA1*, and 12 B6*(Cg)-Tyr*$^{c-2J}$/J mice.

Once mice recovered from head-post surgery, and before testing began, they were placed in a dark room for a minimum of 12 h to acclimate to the dark. Previous studies had a mixed record relative to measuring eye movements in albino mice of various strains (*CD-1; BALB/c; DBA1*) despite the presence of normal structure and function of the retina itself [11,13]. Photophobia is present in the albino mice; thus, it is not surprising that dark adaptation is needed to allow for eye movements to be recorded when using OKR. The ISCAN program (ISCAN, Inc., Woburn, MA) program easily detected the pupil in the *C57BL/6* mice. However, the ISCAN program used for tracking eye movements cannot distinguish an albino mouse's pupil; therefore, in the albino mice a small temporary black ink tattoo was placed on the mouse's eye lateral to, but not overlapping, the pupil for detection by the program. This is an accurate alternative to pupil tracking [12]. The tattoo was created using a mixture of iron oxide and H_2O, then placed onto the eye lateral to the pupil using a blunted needle. No signs of corneal edema occurred in any of these albino mice. Normal eye blinks remove the tattoo after about 45 min. After the tattoo was placed, the mouse's eye movements were recorded while still in the dark room, immobilized using a clamp attached to the head-posts and a tube around their bodies. During testing, the mice were surrounded by a white circular drum with black bars projected onto the white background. The stimulus velocity was 0.5 cycles/second for all testing, and horizontal and vertical eye movements were recorded. Calibration for each mouse was performed before recording eye movements using both no stimuli and stimuli in the ISCAN program to set the detection of the pupil or eye tattoo and the corneal reflection. After a period of rest, pupil tracking was performed first in the absence of the optokinetic stimulus. Following the tracking in the absence of visual stimuli, each mouse was tested using a series of optokinetic stimuli with Michelson contrasts of 10, 25, 50, 75, 100, 200, and 400, and a series of optokinetic stimuli with 0.06, 0.08, 0.10, 0.12, and 0.15 cycles per degree. These series were not randomized, so that each mouse followed the same pattern of contrast variations and differing spatial frequencies. Graphs were generated of the full 86 s of eye tracking that was recorded, and then processed further to show 20 s segments of each trace, to remove tracings where there were a lot of eye blinks or loss of ability to track the tattoo by the video camera momentarily. The ISCAN program measures horizontal and vertical components of the movements of the mouse's pupil or eye tattoo (named the pupil trace), and using a corneal reflection created by a red light near the camera aimed on the mouse eye. To analyze the data from the ISCAN program, raw files of horizontal and vertical movement components were uploaded into a custom program in R (R Foundation for Statistical Computing, Vienna, Austria), where the raw pupil trace was filtered by subtracting the raw corneal reflection trace to remove extra head movements. The average horizontal and vertical positions were calculated for each trace, with each set arbitrarily at zero and −20 respectively for ease of graphic representation. OKR responses were characterized based on published waveform analyses.

RNA-Seq: RNA was isolated from the extraocular muscles (EOM) from 8 mice per genotype, and 4 were chosen for further analysis. An RNA-Seq data set was compiled using tissue obtained from four *C57BL/6*, four *CD-1*, four *BALB/c*, four *DBA1* and, four *B6(Cg)-Tyr*$^{c-2J}$/J mice. EOM from each mouse were collected and prepared for RNA-Seq using the RNeasy Fibrous Tissue Mini Kit (Qiagen, Germantown, MD). After isolation, RNA was assessed for quality using RNA Integrity Number (RIN) score as assayed using an Agilent 2100 Analyzer. The cutoff point for the RNA Integrity Number (RIN) score was 8. These analyses were performed by our Genomic Core facility. RNA-Seq was performed by the University of Minnesota Genomics Center, and all

samples were run on a HiSeq 2500 (Illumina) instrument. The University of Minnesota Informatics Institute analyzed the RNA-Seq output. 2×150bp FastQ paired-end reads for 32 samples (n=22.3 million average per sample) were trimmed using Trimmomatic (v 0.33) enabled with the optional "-q" option; 3bp sliding-window trimming from 3′ end requiring minimum Q30.

Quality control on raw sequence data for each sample was performed with FastQC. Read mapping was performed via Hisat2 (v2.1.0) using the mouse genome (mm10) as reference. Gene quantification was done via Feature Counts for raw read counts. Differentially expressed genes were identified using the edgeR (negative binomial) feature in CLCGWB (Qiagen) using raw read counts.

Genes were qualified as differentially expressed in the EOM between the *C57BL/6, BALB/c, CD-1, DBA1* and, *B6(Cg)-Tyr*$^{c\text{-}2J}$/J mice by having a minimum 2x absolute fold change and a corrected p value (FDR) less than 0.05.

Principal component analysis (PCA) plots were generated, along with a sample-to-sample heat map comparing samples from the EOM of *CD-1, BALB/c*, *DBA1*, *B6(Cg)-Tyr*$^{c\text{-}2J}$/J, and *C57BL/6* mice, to visually validate the RNA-Seq data. Gene plots on log2 transformed counts per million (CPM) values were generated for visualizing different RNA levels of the two genes between the *BALB/c, CD-1*, *DBA1*, *B6*(Cg)-*Tyr*$^{c\text{-}2J}$/J, and *C57BL/6* mice for the EOM. Venny tools were used to numerically visualize genes differentially expressed in the specific tissue analyzed for the 5 genotypes. All data are deposited in GEO and can be found using this accession number: acc=GSE245207.

Immunofluorescence: To validate the RNA-Seq data, the expression of *arrdc2* was examined in the extraocular muscles from adult control, *BALB/c,* and *B6* albino mice (four per genotype). The mice were euthanized with an overdose of carbon dioxide and exsanguination. An orbital exenteration was performed, leaving all rectus muscles and their insertions into the sclera intact. These were embedded in tragacanth gum and frozen using 2-methybutane. Sections were prepared at 12 µm, and stored at −30 °C. Sections were immunostained for ARRDC2 expression using our standard protocol. After rinsing in 0.1M phosphate buffered saline (PBS), sections were blocked for 30 min at room temperature in antibody body that contained 20% goat serum, 0.2% BSA and PBS containing 0.2% Triton-X-100. Without rinsing, the sections were incubated with an antibody to arrdc2 (1:200 in antibody buffer, cat. # NBP3–06285, Novus Biol., Centennial, CO) for 2 h at room temperature. After a PBS rinse, the slides were incubated in a goat anti-rabbit IgG PLUS AF488 (1:1000 in antibody buffer, Cat. # A32731, Invitrogen, Carlsbad, CA) at room temperature for 1 h. The slides were rinsed in PBS and coverslipped using Vectashield antifade mounting medium (H-1700, Vector Labs., Newark, CA). Photographic images were made using a Leica DM4000B fluorescence microscope.

Extraocular muscles were obtained as deidentified surgical waste specimens from children with either idiopathic nystagmus or nystagmus associated with albinism, performed as part of their clinical care by pediatric ophthalmologists. Control muscles were obtained from enucleation due to other diagnoses. The use of these specimens was approved by the appropriate Institutional Review Boards. This study followed the tenets of the Declaration of Helsinki. All specimens were frozen within 1–12 h after surgical removal, stored at -80 °C, and sectioned at 12 µm using a Leica cryostat. Selected sections were then immunostained for ARRDC2 as described in the preceding paragraph.

Ingenuity pathway analysis: Ingenuity Pathway Analysis (IPA; Qiagen, Hilden, Germany) was performed on the differentially expressed gene data sets. These were analyzed for canonical pathways and disease functions. Data are displayed using -log (p value), with $p<0.05$.

RESULTS

Optokinetic nystagmus: We verified that *CD-1*, *BALB/c*, *DBA1*, and B6 albino mice all had nystagmus (Figure 1). In the absence of stimulation in the dark, as expected, the *C57BL/6* did not have any eye movements (Figure 1A). Abnormal jerk waveforms in the absence of stimuli were seen in the albino and hypopigmented mice tested (Figure 1C, E, G, I). In the *DBA1* and B6 albino mice, these jerk movements were seen on the vertical axis also (Figure 1G, I, red trace). In the presence of the moving black and white bars, the normal saw-tooth pattern of the optokinetic reflex was recorded in the *C57BL/6* mice (Figure 1B). Despite 12 h of dark adaptation, the *CD-1* mice showed zero response to the OKR stimulus (Figure 1D). Abnormal OKR waveforms typical of some types of nystagmus were seen in the *BALB/c*, *DBA1*, and B6 albino mice (Figure 1F, H, J).

RNA-seq analysis: RNA-Seq was performed, and a Venn diagram was prepared to identify genes that were differentially expressed in the *CD-1*, *BALB/c*, *DBA1*, and *B6* albino mice compared to the *C57BL/6* for the EOM tissues (Figure 2). For each genotype individually, 242 genes were differentially expressed by the B6 albino EOM, 293 genes were differentially expressed by the *BALB/c* EOM, 399 genes were differentially expressed by the *DBA/1* EOM, and 225 genes were differentially expressed by the *CD-1* EOM. After the combinatorial analysis, 14 genes were identified that were differentially expressed across all 3 albino and

hypopigmented mice (Figure 2). These were: *arrdc2, Ccl8, Cd209 g, Cox16, Ddit4, Gbp10, Gm9994, H2-K2, H2-Q5, Kcnk3, mss51, pnmt, Slc6a12,* and *Tmem171.* We include a summary of the main findings for all 14 genes identified, including fold change, uncorrected p values, FDR-adjusted p values (Table 1) and mean values (Table 2).

Principal component analysis of the RNA-Seq data from 4 samples of the EOM from each of the 5 genotypes was performed to assess validity and give a bigger picture of the overall differences of these genotypes compared to each other in the EOM (Figure 3). The first principal component showed a tight clustering of all genotypes, with the *CD-1* and *DBA/1* genotypes showing a slight divergence from the *BALB/c*. The second principal component analysis separated the data into one group consisting of the two mouse genotypes on the *C57BL/6* background from the albinos and hypopigmented mice.

The sample-to-sample distance heat map for the RNA-Seq data for the EOM for all 5 genotypes was generated to show which samples were similar to each other relative to their gene expression (Figure 4). The heat map for the extraocular muscles shows that the pigmented control mice (C), the B6 albino (Ty), and the hypopigmented mice have

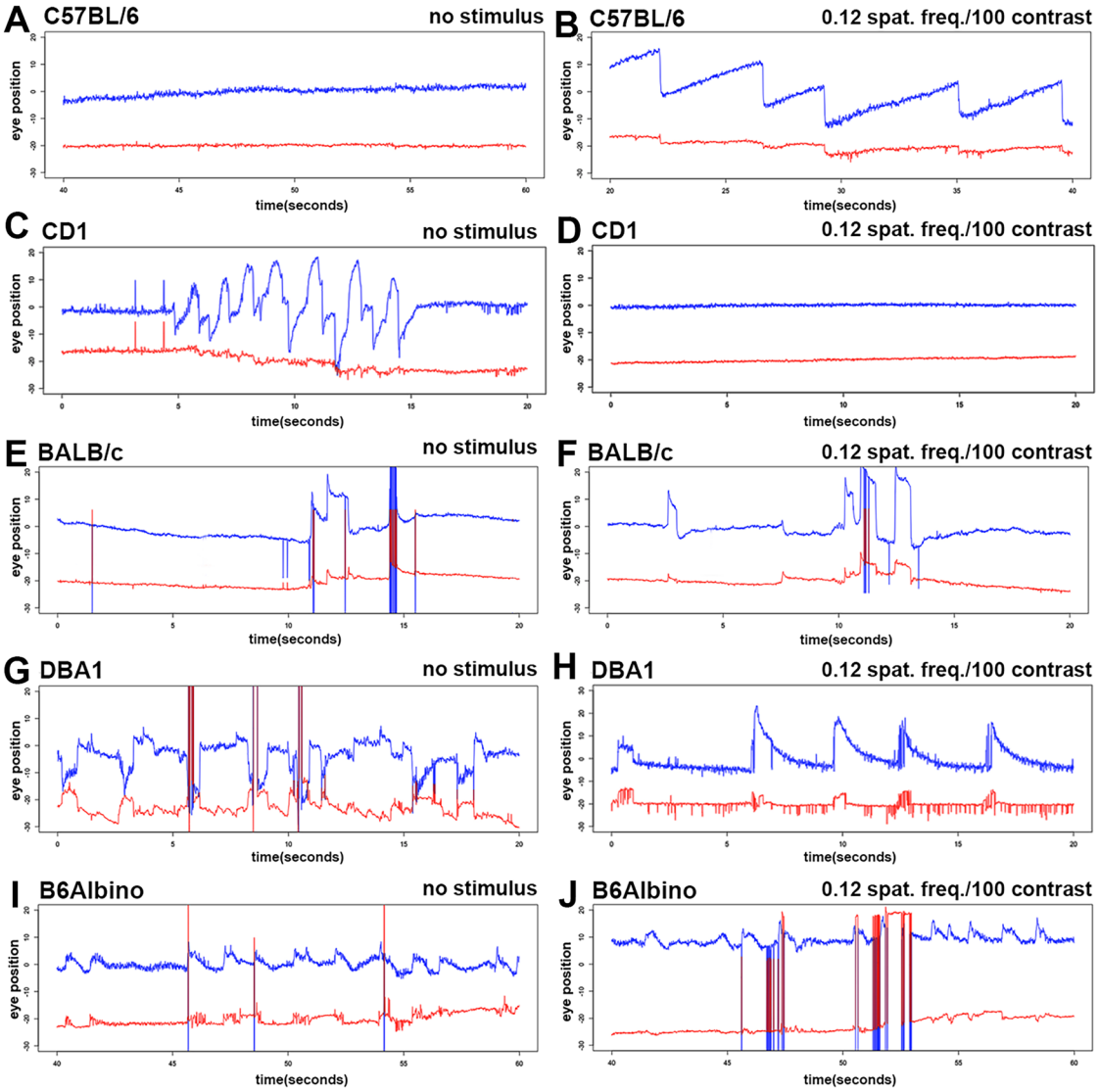


Figure 1. Optokinetic reflex traces. Optokinetic reflex traces from (**A**, **B**) *C57BL/6* mice, (**C**, **D**) *CD-1* mice, (**E**, **F**) *BALB/c* mice, (**G**, **H**) *DBA1* mice, and (**I**, **J**) *B6(Cg)-Tyr^{c-2J}/J* (B6 albino) mice. (**A**, **C**, **E**, **G**, **I**) OKR in the absence of a stimulus and (**B**, **D**, **F**, **H**, **J**) OKR in the presence of moving black bars at a spatial frequency of 0.12 and at contrast 100.

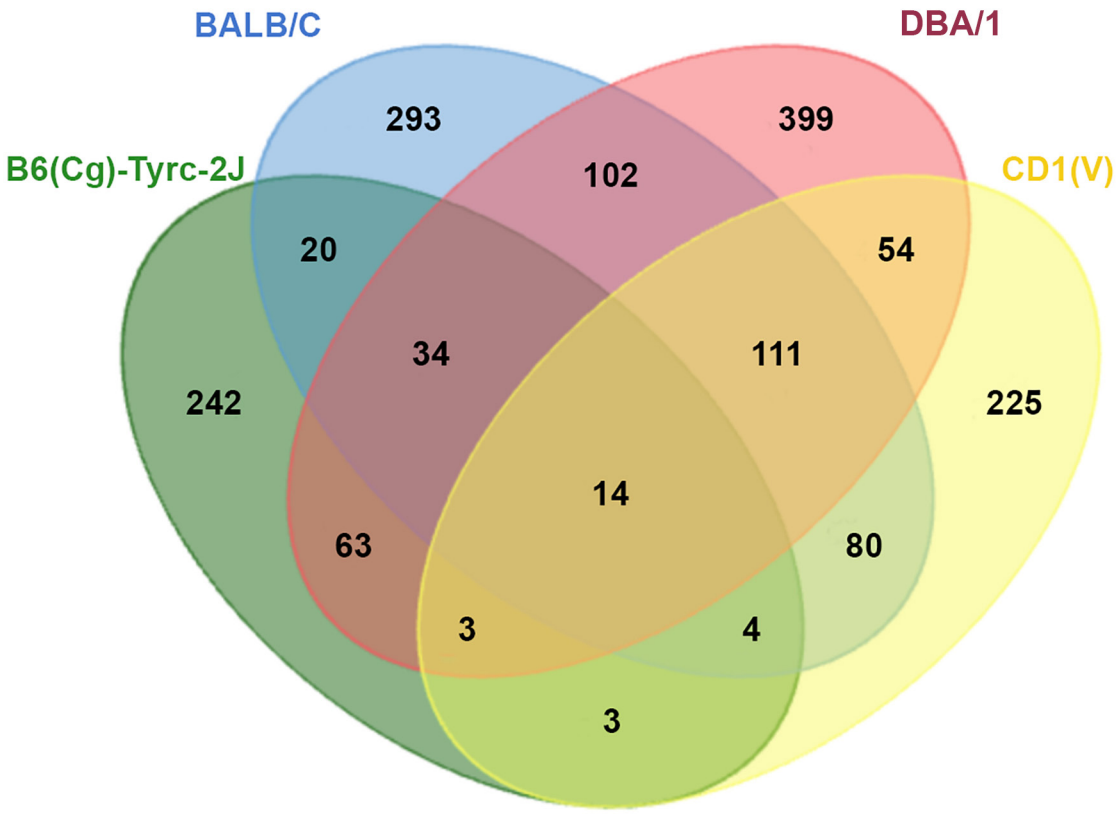


Figure 2. Comparison Venn graph. Venn graph for EOM comparing *C57BL/6* expressed genes to the combined differentially expressed genes of all albino and hypopigmented strains identified genes. When the genes expressed by the extraocular muscle tissue in *C57BL/6* mice were compared to the genes of all three albino and hypopigmented mice, fourteen genes were found to be differentially expressed.

similarities, as do the two groups of albino mice, the *BALB/c* (B) and *CD-1* (V).

From the 14 differentially expressed genes in the *CD-1*, *BALB/c*, *DBA1*, and B6 albino mice compared to the *C57BL/6* for the EOM tissues we chose to examine *arrdc2* and *mss51* for further gene expression analysis and *arrdc2* for immunohistochemical validation. The *arrdc2* gene is a mechanosensitive gene and its induction in myotubes is sufficient to produce thinner myotubes and a transcriptional landscape consistent with muscle atrophy and disuse [14]. In addition, based on the rationale that INS has a childhood onset and surgical muscle samples indicated decreased innervation, *arrdc2* might play a role in control of nerve outgrowth and communication between the ocular motor neurons and the EOM. The *mss51* gene modulates skeletal muscle mitochondrial respiration and fatigue resistance [15]. From our RNA-Seq data we calculated gene expression for each of these genes (Figure 5). In the EOM of *CD-1*, *BALB/c*, *DBA1*, and B6 albino mice *arrdc2* had a smaller gene count expression compared to the gene expression in the *C57BL/6* mice. In the EOM of *CD-1*, *BALB/c*, *DBA1*, and B6 albino mice *mss51* had a larger gene count expression compared to the gene expression in the *C57BL/6* mice.

Immunofluorescence: We validated this difference in gene expression of *arrdc2* through immunofluorescent staining of EOM for expression of the ARRDC2 protein in *C57BL/6* EOM (Figure 6A), BALB/c EOM (Figure 6B), and B6 albino EOM (Figure 6C). ARRDC2 protein expression was decreased in the albino EOM compared to the level of expression in the pigmented *C57BL/6* EOM, with the EOM from the B6 albino showing expression patterns qualitatively decreased compared to the control but with less ubiquitous immunostaining of all myofibers. This confirms our gene expression data from our RNA-Seq experiment. We further validated the association of *arrdc2* expression in EOM from human age-matched controls (Figure 7A), surgical waste EOM from an age-matched individual with strabismus (Figure 7B), surgical waste EOM from individuals diagnosed with idiopathic infantile nystagmus syndrome (Figure 7C,D), and an individual with nystagmus whose genetic testing showed they

had OCA1-type albinism (Figure 7E). All of the specimens from individuals with nystagmus showed decreased levels of ARRDC2 expression compared to both the control EOM and the EOM tissue from an individual with strabismus but no nystagmus.

IPA pathways: Pathway analysis examining all 3 albino and the hypopigmented mice identified several pathways that were uniformly up- or downregulated in all 4 mouse strains with nystagmus, allowing us to separate those pathways potentially involved just with albinism (Figure 8). For canonical pathways, only downregulated canonical pathways in all four mice genotypes were seen. These include DHCR24 signaling and cardiac hypertrophy signaling. DHCR24 (24-dehydrocholesterol reductase) has been linked to maintaining muscle size [16], which would lead to the prediction that its reduction in the EOM from individuals with nystagmus could lead to decreased or altered muscle mass. Similarly, the cardiac hypertrophy signaling pathway

Table 1. P-value, expression fold change, and FDR p-value corrections for all albino and hypopigmented genotypes compared to C57BL/6 for each DEG.

	C57BL/6 vs BALB/c			C57BL/6 vs CD-1		
Gene	P-value	Fold change	FDR p-value correction	P-value	Fold change	FDR p-value correction
Arrdc2	2.34E-12	-5.54031	6.43E-10	6.17E-15	-9.08697	8.38E-12
Ccl8	2.11E-06	3.675286	0.000143	0.000183	2.915059	0.01176
Cd209g	9.49E-06	2.424562	0.000521	0.000137	2.228761	0.009178
Cox16	0.000946	-2.49757	0.021256	0.000779	-2.77954	0.033556
Ddit4	4.76E-06	-3.48269	0.000284	0.019807	-1.98641	0.269248
Gbp10	2.62E-31	19.66371	5.34E-28	4.99E-12	5.562468	2.83E-09
Gm9994	1.23E-05	-4.1104	0.000642	6.95E-05	-4.0711	0.005353
H2-K2	0.000115	-3.39549	0.004085	2.41E-08	-8.25443	7.10E-06
H2-Q5	0.001133	-3.21069	0.024395	0.001123	-3.65563	0.04273
Kcnk3	1.84E-13	3.553167	6.32E-11	1.46E-12	3.578158	1.05E-09
Mss51	1.42E-06	4.047126	0.000101	3.79E-05	3.463585	0.003386
Pnmt	1.62E-07	-5.69589	1.53E-05	1.29E-07	-7.02292	3.12E-05
Slc6a12	3.98E-06	3.533055	0.000244	0.000345	2.783017	0.018797
Tmem171	5.21E-11	4.5255	1.14E-08	0.000151	2.476823	0.010071
	C57BL/6 vs DBA1			C57BL/6 vs B6 albino		
Gene	P-value	Fold change	FDR p-value correction	P-value	Fold change	FDR p-value correction
Arrdc2	1.96E-12	-5.55821	4.92E-10	3.87E-05	-2.62162	0.003011
Ccl8	6.87E-12	6.882349	1.51E-09	0.000323	2.664441	0.012903
Cd209g	5.43E-06	2.478417	0.000269	0.000176	2.114531	0.008592
Cox16	0.000456	2.530699	0.009901	0.004507	2.112328	0.066257
Ddit4	2.16E-05	-3.16578	0.000867	0.00212	-2.27869	0.041519
Gbp10	8.23E-08	3.533857	7.31E-06	0.000196	2.391471	0.009264
Gm9994	1.23E-05	-4.13102	0.000541	0.001211	-2.758	0.029543
H2-K2	1.22E-06	-4.85565	7.36E-05	0.004603	2.290424	0.067076
H2-Q5	5.58E-08	4.825665	5.14E-06	2.15E-06	3.968977	0.000372
Kcnk3	4.56E-18	4.489644	2.14E-15	2.97E-09	2.754713	1.53E-06
Mss51	3.29E-07	4.411024	2.41E-05	0.000412	2.751192	0.015255
Pnmt	5.01E-05	-3.60068	0.001714	0.000436	-3.00835	0.015868
Slc6a12	1.71E-07	4.079099	1.36E-05	0.000956	2.513539	0.025334
Tmem171	9.17E-08	3.381336	7.97E-06	3.95E-13	5.339819	6.02E-10

Table 2. Mean gene expression for across all genotypes for each DEG.

Gene	C57BL/6- Means	BALB/c - Means	CD-1 - Means	DBA1 - Means	B6 albino - Means
Arrdc2	991.00	150.75	144.00	183.75	364.25
Ccl8	60.00	182.25	230.67	420.00	154.25
Cd209g	108.00	234.50	332.33	280.00	224.25
Cox16	84.00	29.75	42.33	223.25	171.75
Ddit4	1097.75	276.75	707.00	362.50	461.00
Gbp10	68.00	1145.75	509.67	250.00	157.75
Gm9994	53.00	11.75	17.67	13.25	18.50
H2-K2	57.25	14.75	9.33	12.00	126.50
H2-Q5	15.25	4.25	5.67	78.00	58.50
Kcnk3	160.25	529.50	790.33	761.50	436.75
Mss51	77.25	274.75	343.33	355.00	207.75
Pnmt	102.25	15.00	19.33	29.00	31.75
Slc6a12	10.25	32.50	39.33	44.25	25.75
Tmem171	48.50	200.00	164.67	171.00	248.50

lists a large number of molecules that are known to be involved in regulating both EOM anatomy and physiologic properties, to include decreased levels of insulin-like growth factor 1 and altered levels of cardiac specific myosin heavy chains – known to be expressed in the EOM [17-19]. In the pathway analysis related to Diseases and Function, downregulated pathways included sepsis, diabetes mellitus, fatty acid metabolism, and energy homeostasis. Many of the associated molecules overlap between these four pathways, and include insulin-like growth factor 1 and other neurotrophic factors known to play a role in maintenance of normalcy in the EOM. Interestingly, upregulated disease pathways are related to seizures and to neurologic signaling. Molecules associated with these two pathways include the muscarinic cholinergic receptor, the dopamine receptor, and multiple myosin heavy chain isoforms including the EOM-specific myosin. This is interesting in light of the changes seen in the EOM from individuals with nystagmus, such as increased centralized nuclei,

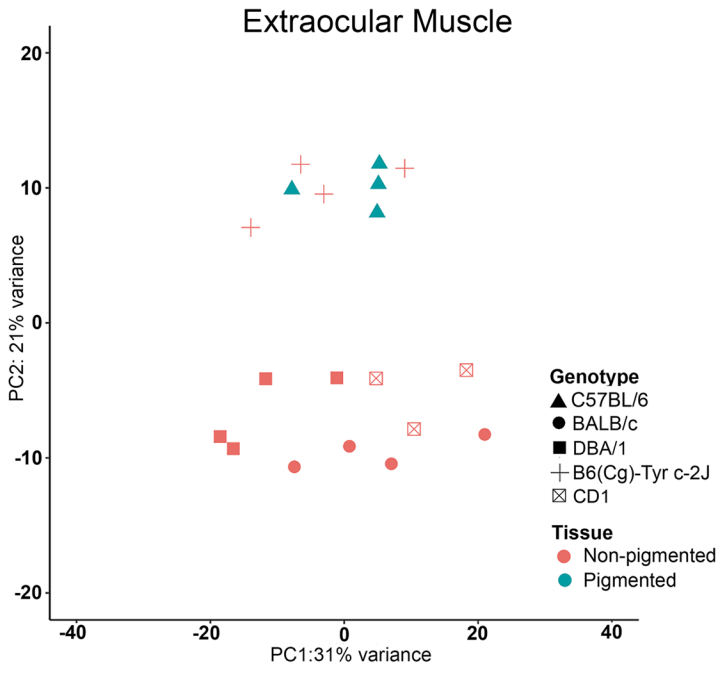


Figure 3. Principal component analysis. Principal component analysis for EOM tissues created using a DESeq2 package in R to define the first two principal components comparing samples from the RNA-seq sequences generated.

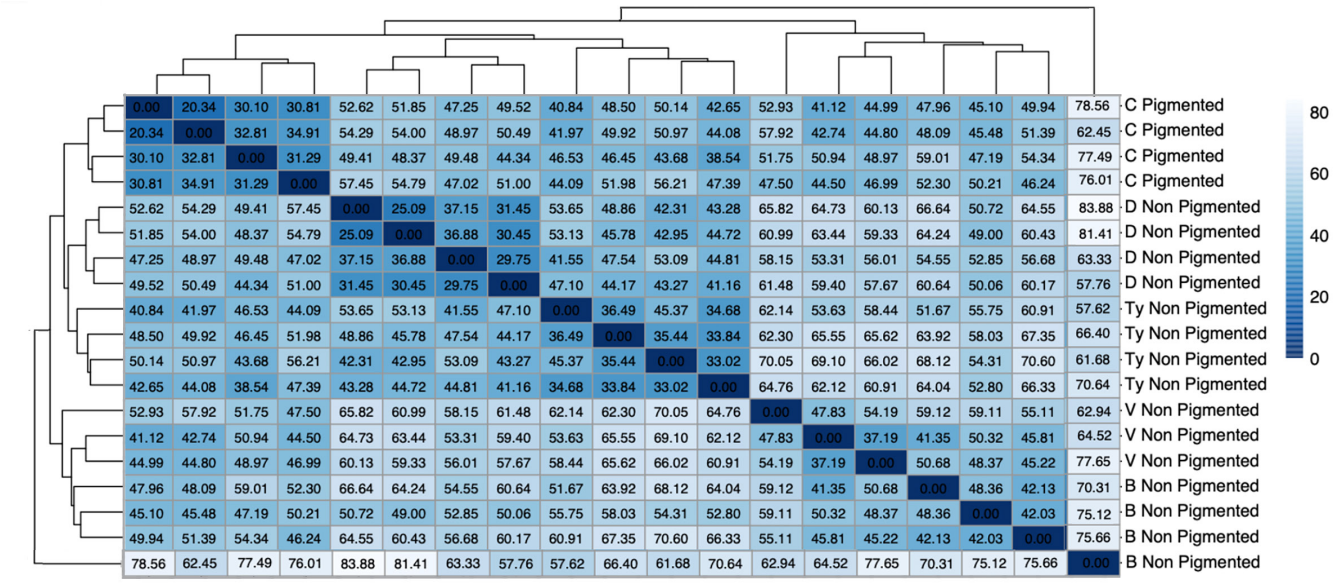


Figure 4. Comparison heatmap. Heatmap of EOM from *C57BL/6* versus all albino tissues. *C57BL/6* is **C**; *BALB/c* is **B**; *CD-1* is V, *B6(Cg)-Tyr*$^{c-2J}$*/J* is Ty, and the hypopigmented *DBA/1J mouse* is **D**.

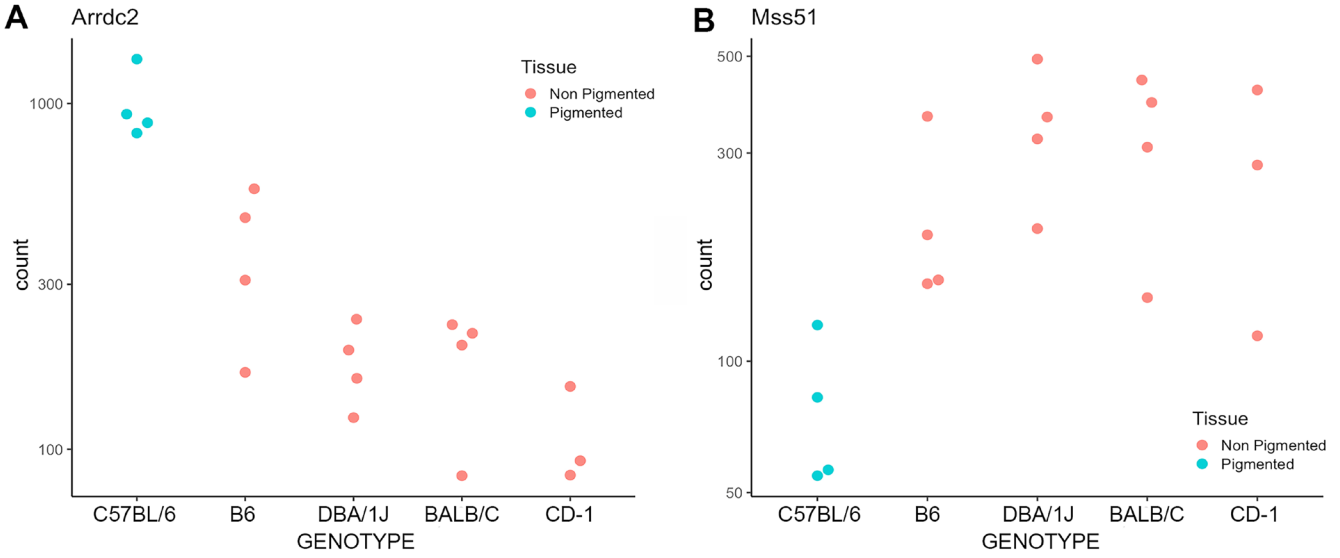


Figure 5. Gene count plots for *arrdc2* and *mss51*. **A**: Gene count plot for *arrdc2* across all genotypes for gene expression in EOM. Each point represents a single sample from each of the 5 genotypes. Note that the y-axis is a log scale. These were created using a DESeq program in R. *Arrdc2* expression is downregulated in the EOM of all albino and hypopigmented mice compared to the *C57Bl/6* pigmented control mice. **B**: Gene count plot for *mss51* across all genotypes for gene expression in EOM. Each point represents a single sample from each of the 5 genotypes. Note that the y-axis is a log scale. These were created using a DESeq program in R. *Mss51* is upregulated in the EOM of all albino and hypopigmented mice compared to the *C57BL/6* pigmented control mice.

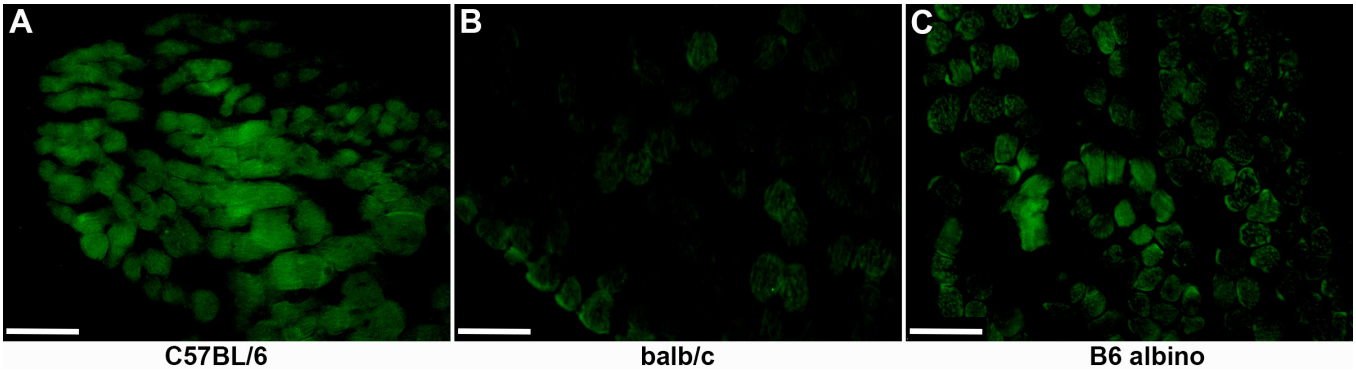


Figure 6. Immunofluorescent staining for ARRDC2. Immunofluorescent staining of EOM from mice for expression of ARRDC2 in (**A**) *C57BL/6* EOM, (**B**) BALB/c EOM, and (**C**) B6 albino EOM. ARRDC2 protein expression is decreased in the albino EOM compared to the level of expression in the pigmented *C57BL/6* EOM.

– indicative of muscle denervation/reinnervation – decreased nerve fiber density [20] and abnormally small and immature neuromuscular junctions [21]. When these molecules are validated for their expression and biologic function, they may provide for identification of potentially druggable target molecules.

DISCUSSION

All the albino and hypopigmented mice displayed nystagmus as defined by the jerk waveforms seen in the absence of OKR stimulus. All but the *CD-1* mice showed abnormal waveforms in response to the OKR stimulus – rotating white and black bars – confirming previous studies [11,12]. Unexpectedly, all

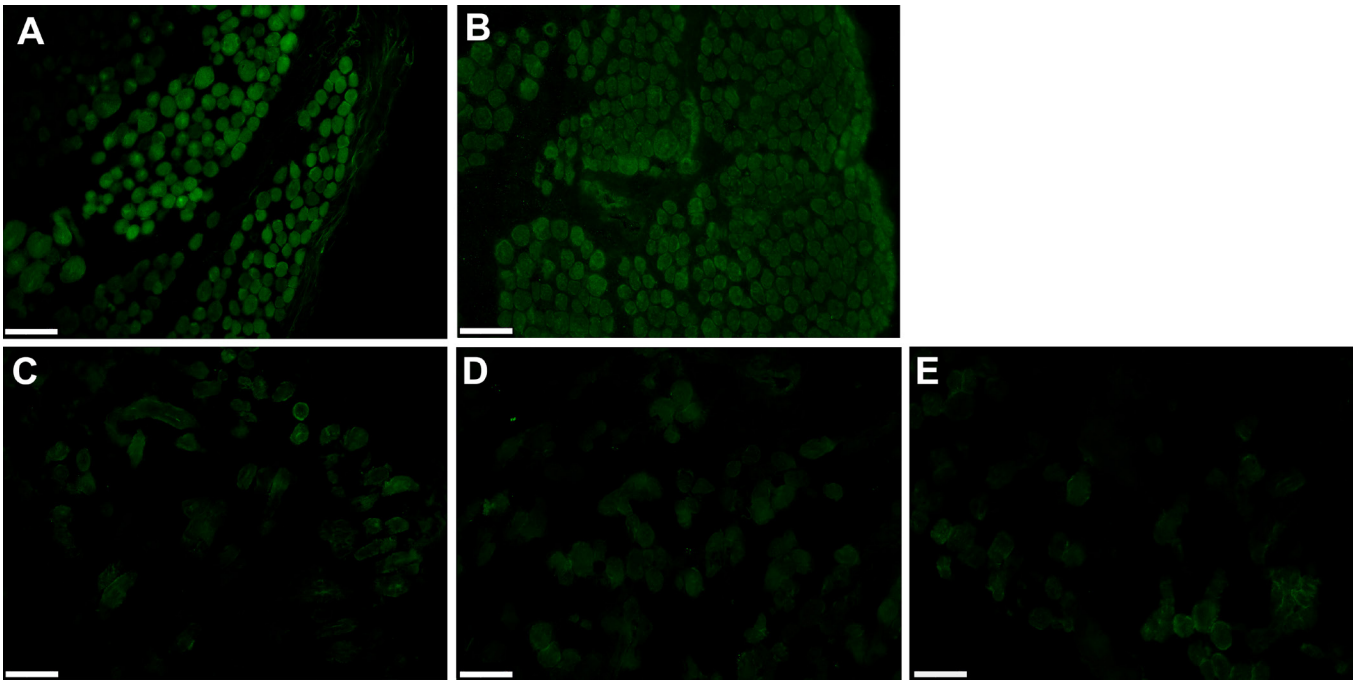


Figure 7. Immunofluorescent staining for ARRDC2 in human EOM. Immunofluorescent staining for ARRDC2 of human surgical waste extraocular muscles. **A**: control EOM, (**B**) EOM from a strabismic individual, and (**C**-**E**) EOM from three separate individuals diagnosed with INS. **C** and **D** represent individuals with idiopathic infantile nystagmus syndrome and **E** represents an individual with nystagmus whose genetic testing indicated they had OCA1-type albinism.

the *CD-1* mice tested had no visible eye movements in the presence of the OKR stimulus.

It is well known that INS is known to be associated with sensory afferent defects such as albinism and optic nerve hypoplasia [22-24]. However, recent studies have demonstrated that INS is also associated with motor nerve outgrowth defects [4,5], neuromuscular junction abnormalities [20,21], and muscle-specific mutations [9,10], and that these abnormalities compared to normal controls are present in the mouse models of INS before eye opening [25,26]. There is no cure for INS, with its known associated decreases in visual acuity in these children. Unfortunately, development of effective treatments for idiopathic and albinism-associated INS is hampered by our lack of understanding of the primary and compensatory changes that cause these uncontrolled oscillatory movements of the eyes.

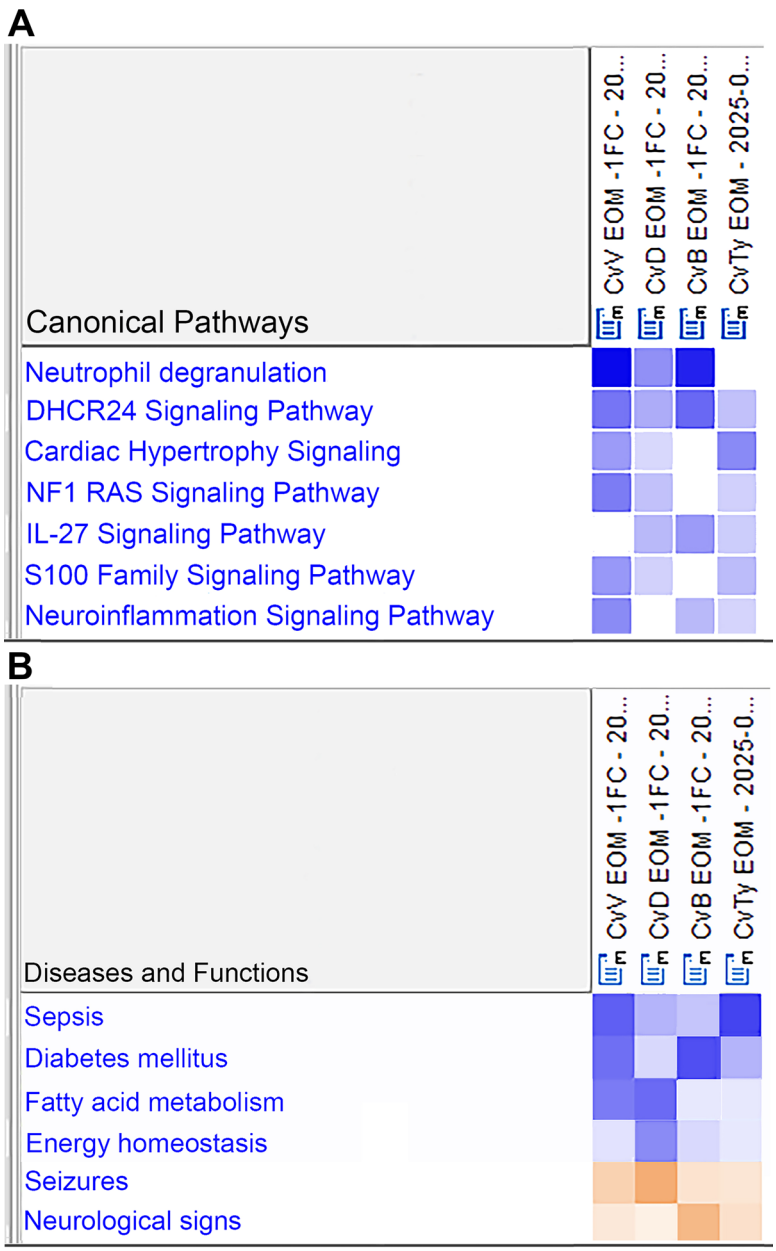


Figure 8. Canonical and disease pathway analyses. **A**: Pathway comparison analysis for major canonical pathway changes common to all albino and hypopigmented EOM compared to controls. **B**: Pathway analysis showing major pathway changes common to all albino and hypopigmented EOM compared to controls related specifically to disease and biologic functions of muscle.

Our combinatorial RNA-Seq approach allowed us to identify potential new druggable targets to treat INS. One of the albino mouse strains used in this study, the B6 albino mice, is genetically identical to *C57BL/6* mice except for a mutation in the *tyrosinase* gene, making them phenotypically albino [27]. As we previously demonstrated, they have nystagmus as their eye movements are abnormal with erratic eye oscillations [12]. This makes them an excellent albino model to include in this study, as this allowed a focus on the gene expression comparisons that are hypothesized to be specific for nystagmus, rather than solely the result of albinism or hypopigmentation, when compared to a *C57BL/6* pigmented mouse. Using a combinatorial RNA-Seq approach to analyze the gene expression of the EOM from the albino and hypopigmented mice with nystagmus compared to a pigmented mouse resulted in the identification of only 14 genes that were differentially expressed between the mice with nystagmus and the control mouse EOM. One gene of particular interest is *arrdc2*, whose expression was downregulated in the INS samples from our analysis. This gene has been linked to controlling muscle mass in aging, disuse atrophy, and reloading [14,28]. Upregulation in the expression of ARRDC2 has also been linked to increasing neuroplasticity [29], and thus its downregulation may play a role in the reduced innervation and/or immature neuromuscular junctions found in the EOM surgical samples from INS individuals. Another of the differentially expressed genes, *mss51*, was found to be upregulated in the EOM of the mice with nystagmus. Studies have shown that alterations in MSS51expression alters endurance and fatigue resistance, and its deletion can increase muscle mass [30] and in the skeletal muscles of the *mdx* mouse, a mouse model for Duchenne muscular dystrophy, gene disruption resulted in increased endurance and decreased fatigue [15]. As MSS51 expression is increased in the EOM from our mouse models with nystagmus, it may be playing a role in their altered muscle function. Future studies can examine mouse models where these genes have been either constitutively or conditionally knocked-out or upregulated to determine if loss or gain of expression is associated with nystagmus. If animal models with either of these two genes altered have nystagmus, it will support the hypothesis these they play a potentially causative or maintenance role in development of INS.

It will be very interesting to investigate the potential role of the other 12 identified genes from this analysis in the development or maintenance of nystagmus. Several these genes also have known roles in the function of skeletal muscle. *Ccl8* (chemokine c-c motif ligand 8) is generally known for its role in immune system function, including cell recruitment, inflammation, and disease progression [31]. However, recent studies have demonstrated that it is a negative regulator of regeneration in skeletal muscle, and it is expressed specifically on PAX7-positive muscle satellite cells [32]. Expression of CCL8 was increased in the EOM from the mice with nystagmus, which would be predicted to result in decreased muscle fiber size and decreased myofiber turnover [33]. The gene *Ddit4* (DNA damage-inducible transcript 4) can play an active role in skeletal muscle building by regulating levels of the protein-building molecule mTORC1 [34]. Its expression was decreased in the EOM from mice with nystagmus, which would be predicted to reduce the formation or remodeling of muscle fibers [35]. Another identified gene was *kcnk3* (potential channel subfamily K member 3), which was upregulated in the EOM from the mice with nystagmus. As a potassium leak channel, it allows K+ to flow out of cells, controlling rate of muscle cell contraction [36]. It plays an important role in cardiac muscle, and it is normally expressed at low levels in skeletal muscle. However, parts of the heart and the extraocular muscles develop from the same embryonic tissue [37]. In addition, the EOM express several “cardiac-specific” molecules including the two cardiac myosin heavy chain isoforms [38] and cardiac troponin [39], among others. Considering its role in controlling heart contractility, it would be important to determine if the extraocular muscles normally express KCNK3, as well as determine its function in the EOM from normal individuals as well as those with nystagmus. The gene *cox16* is a cytochrome c oxidase (complex IV), and is highly active in skeletal muscle mitochondria [40]. Decreased levels in the EOM from the mice with nystagmus suggest that the EOM in individuals with nystagmus may be experiencing an energy deficit – reducing the energy they need for normal contraction. *Pnmt* (phenylethanolamine N-methyltransferase) is an enzyme involved in the synthesis of epinephrine, and can cause potentiation of responses in skeletal muscle [41]. One hypothesis for the effect of decreased expression of this enzyme in the EOM from the mice with nystagmus, could be reduced muscle contractile force [42]. *Slc6a12* (solute carrier family 6 member 12 or sodium- and chloride-dependent betaine transporter) is a transporter in the osmolyte pathway, and it has been described as upregulated in regenerating skeletal muscle, playing a protective role [43,44]. Its potential role in the EOM is unclear. Two genes, *Tmem171* (transmembrane protein 171), which is upregulated in the EOM of the mice with nystagmus, and *Gm9994*, which is downregulated, have no known skeletal muscle function.

The rest of the other differentially expressed genes are involved in immune system function. These include *cd209 g*, which within skeletal muscle acts as an immune sensor for recognizing cellular debris and regulating local inflammation [45], *gbp10* (gualylate-binding protein 10), which presumably

plays a role in the innate immune responses in the EOM [46], and H2-K2 and H2-Q5, both involved in antigen presentation. There is evidence to suggest that the immune cell populations with the EOM differ from that of limb skeletal muscle [47], but more work is needed to understand in more detail the immune system differences within the EOM, both in normal EOM and in individuals with nystagmus.

Collectively, this combinatorial RNA-seq approach enables the identification of genes not previously associated with INS. The function of ARRDC2 and MSS51 molecules within the EOM remains unknown, and further studies are needed for the validation of their expression levels and biologic functions. However, these studies support the view that this combinatorial approach for identification of new genes whose expression is altered in nystagmus has the potential to uncover novel molecules important for nystagmus development and/or maintenance. When validated for their biologic function in vitro and in vivo, could also provide insight into potentially druggable targets that may be effective in treating the underlying basis for the uncontrolled eye oscillations in nystagmus.

ACKNOWLEDGMENTS

This manuscript is the result of funding in part by the National Institute of Health (NIH) Public Access Policy. Through acceptance of this federal funding, NIH has been given a right to make this manuscript publicly available in PubMed Central upon the Official Date of Publication, as defined by NIH. R01EY15313 (LKM), T32EY025187 (LLJ), and T32AR007612 (LLJ), and NIH T32AR007612 (LLJ), and University of Minnesota Internal Sabbatical.

This is an open-access article distributed under the terms of the Creative Commons Attribution-NonCommercial-NoDerivatives 4.0 International License, which permits reusers to copy and distribute the material in any medium or format in unadapted form only, for noncommercial purposes only, and only so long as attribution is given to the creator. CC BY-NC-ND includes the following elements: BY: credit must be given to the creator. NC: Only noncommercial uses of the work are permitted. ND: No derivatives or adaptations of the work are permitted.

REFERENCES

1. Papageorgiou E, McLean RJ, Gottlob I. Nystagmus in childhood. Pediatr Neonatol 2014; 55:341-51. [PMID: 25086850].
2. Nash DL, Diehl NN, Mohney BG. Incidence and types of pediatric nystagmus. Am J Ophthalmol 2017; 182:31-4. [PMID: 28734813].
3. Thomas MG, Maconachie G, Sheth V, McLean RJ, Gottlob I. Development and clinical utility of a novel diagnostic nystagmus gene panel using targeted next-generation sequencing. Eur J Hum Genet 2017; 25:725-34. [PMID: 28378818].
4. Tarpey P, Thomas S, Sarvananthan N, Mallya U, Lisgo S, Talbot CJ, Roberts EO, Awan M, Surendran M, McLean RJ, Reinecke RD, Langmann A, Lindner S, Koch M, Jain S, Woodruff G, Gale RP, Bastawrous A, Degg C, Droutsas K, Asproudis I, Zubcov AA, Pieh C, Veal CD, Machado RD, Backhouse OC, Baumber L, Constantinescu CS, Brodsky MC, Hunter DG, Hertle RW, Read RJ, Edkins S, O'Meara S, Parker A, Stevens C, Teague J, Wooster R, Futreal PA, Trembath RC, Stratton MR, Raymond FL, Gottlob I. Mutations in FRMD7, a newly identified member of the FERM family, cause X-linked idiopathic congenital nystagmus. Nat Genet 2006; 38:1242-4. [PMID: 17013395].
5. Betts-Henderson J, Bartesaghi S, Crosier M, Lindsay S, Chen HL, Salomoni P, Gottlob I, Nicotera P. The nystagmus-associated FRMD7 gene regulates neuronal outgrowth and development. Hum Mol Genet 2010; 19:342-51. [PMID: 19892780].
6. Huettl R-E, Eckstein S, Stahl T, Petricca S, Ninkovic J, Götz M, Huber AB. Functional dissection of the Pax6 paired domain: Roles in neural tube patterning and peripheral nervous system development. Dev Biol 2016; 413:86-103. [PMID: 26187199].
7. Tzoulaki I, White IMS, Hanson IM. PAX6 mutations: genotype-phenotype correlations. BMC Genet 2005; 6:27-[PMID: 15918896].
8. Oetting WS, King RA. Molecular basis of albinism: mutations and polymorphisms of pigmentation genes associated with albinism. Hum Mutat 1999; 13:99-115. [PMID: 10094567].
9. Johnson LL, Kueppers RB, Shen EY, Rudell JC, McLoon LK. Development of nystagmus in the absence of MYOD expression in the extraocular muscles. Invest Ophthalmol Vis Sci 2021; 62:3-[PMID: 34617961].
10. Johnson LL, Hebert S, Kueppers RB, McLoon LK. Nystagmus associated with the absence of MYOD expression across the lifespan in extraocular and limb muscles. Invest Ophthalmol Vis Sci 2023; 64:24-[PMID: 37703038].
11. Traber GL, Chen CC, Huang YY, Spoor M, Roos J, Frens MA, Straumann D, Grimm C. Albino mice as an animal model for infantile nystagmus syndrome. Invest Ophthalmol Vis Sci 2012; 53:5737-47. [PMID: 22789924].
12. Johnson LL, Abrahante JE, McLoon LK. Nystagmus in the *B6(CG)Tyr(c-2J)/J* albino mouse: A functional and RNA-Seq analysis. Invest Ophthalmol Vis Sci 2024; 65:26-[PMID: 38206276].
13. Puk O, Dalke C, Hrabé de Angelis M, Graw J. Variation of the response to the optokinetic drum among various strains of mice. Front Biosci 2008; 13:6269-75. [PMID: 18508659].
14. Laskin GR, Cabrera AR, Greene NP, Tomko RJ Jr, Vied C, Gordon BS. The mechanosensitive gene *arrestin domain containing 2* regulates myotube diameter with direct

implications for disuse atrophy with aging. Am J Physiol Cell Physiol 2024; 326:C768-83. [PMID: 38314723].

15. Rovira Gonzalez YI, Moyer AL, LeTexier NJ, Bratti AD, Feng S, Sun C, Liu T, Mula J, Jha P, Iyer SR, Lovering RM, O'Rourke B, Noh HL, Suk S, Kim JK, Essien Umanah GK, Wagner KR. Mss51 deletion enhances muscle metabolism and glucose homeostasis in mice. JCI Insight 2019; 4:e122247[PMID: 31527314].

16. Zhang R, Peng S, Zhang X, Huang Z, Pan X. High mRNA expression of 24 dehydrocholesterol reductase (CHCR24) in the treatment of doxorubicin-induced heart failure in rats. Int J Mol Sci 2025; 26:312-[PMID: 39796168].

17. Feng CY, von Bartheld CS. Expression of insulin-like growth factor 1 isoforms in the rabbit oculomotor system. Growth Horm IGF Res 2011; 21:228-32. [PMID: 21703892].

18. Rind HB, von Bartheld CS. Target-derived cardiotrophin-1 and insulin-like growth factor-I promote neurite growth and survival of developing oculomotor neurons. Mol Cell Neurosci 2002; 19:58-71. [PMID: 11817898].

19. Wieczorek DF, Periasamy M, Butler-Browne GS, Whalen RG, Nadal-Ginard B. Co-expression of multiple myosin heavy chain genes, in addition to a tissue-specific one, in extraocular musculature. J Cell Biol 1985; 101:618-29. [PMID: 3894379].

20. Berg KT, Hunter DG, Bothun ED, Antunes-Foschini R, McLoon LK. Extraocular muscles in patients with infantile nystagmus: adaptations at the effector level. Arch Ophthalmol 2012; 130:343-9. [PMID: 22411664].

21. McLoon LK, Willoughby CL, Anderson JS, Bothun ED, Stager D Jr, Felius J, Lee H, Gottlob I. Abnormally small neuromuscular junctions in the extraocular muscles from subjects with idiopathic nystagmus and nystagmus associated with albinism. Invest Ophthalmol Vis Sci 2016; 57:1912-20. [PMID: 27092717].

22. Creel D, Spekreijse H, Reits D. Evoked potentials in albinos: efficacy of pattern stimuli in detecting misrouted optic fibers. Electroencephalogr Clin Neurophysiol 1981; 52:595-603. [PMID: 6172258].

23. Creel DJ, Summers CG, King RA. Visual anomalies associated with albinism. Ophthalmic Paediatr Genet 1990; 11:193-200. [PMID: 2280977].

24. Guibal C, Baker GE. Abnormal axons in the albino optic tract. Invest Ophthalmol Vis Sci 2009; 50:5516-21. [PMID: 19628745].

25. Vemula SK, Kim SA, Muvavarirwa T, Bell JL, Whitman MC. Impaired extraocular muscle innervation is present before eye opening in a mouse model of infantile nystagmus syndrome. Invest Ophthalmol Vis Sci 2022; 63:4-[PMID: 36083589].

26. Vemula S, Osman A, Yang X, Aronchik G, Martinez Sanchez M, Meher N, Whitman MC. Disrupted motor neuron and neuromuscular junction development in an albino mice model of infantile nystagmus. Invest Ophthalmol Vis Sci 2025; 66:25-[PMID: 40637510].

27. Townsend D, Witkop CJ Jr, Mattson J. Tyrosinase subcellular distribution and kinetic parameters in wild type and C-locus mutant *C57BL/6J* mice. J Exp Zool 1981; 216:113-9. [PMID: 6793688].

28. Gordon BS, Rossetti ML, Eroshkin AM. Arrdc2 and Arrdc3 elicit divergent changes in gene expression in skeletal muscle following anabolic and catabolic stimuli. Physiol Genomics 2019; 51:208-17. [PMID: 31002587].

29. Jefsen OH, Elfving B, Wegener G, Müller HK. Transcriptional regulation in the rat prefrontal cortex and hippocampus after a single administration of psilocybin. J Psychopharmacol 2021; 35:483-93. [PMID: 33143539].

30. Mousa MG, Vuppaladhadiam L, Kelly MO, Pietka T, Ek S, Shen KC, Meyer GA, Finck BN, Brookheart RT. Site-1 protease inhibits mitochondrial respiration by controlling the TGF-β target gene *Mss51*. Cell Rep 2023; 42:112336[PMID: 37002920].

31. Van Damme J, Proost P, Lenaerts JP, Opdenakker G. Structural and functional identification of two human, tumor-derived monocyte chemotactic proteins (MCP-2 and MCP-3) belonging to the chemokine family. J Exp Med 1992; 176:59-65. [PMID: 1613466].

32. Boss-Kennedy A, Kim D, Barai P, Maldonado C, Reyes-Ordoñez A, Chen J. Muscle cell-derived Ccl8 is a negative regulator of skeletal muscle regeneration. FASEB J 2024; 38:e23841[PMID: 39051762].

33. McLoon LK, Rowe J, Wirtschafter J, McCormick KM. Continuous myofiber remodeling in uninjured extraocular myofibers: myonuclear turnover and evidence for apoptosis. Muscle Nerve 2004; 29:707-15. [PMID: 15116375].

34. Miyazaki M, Esser KA. Cellular mechanisms regulating protein synthesis and skeletal muscle hypertrophy in animals. J Appl Physiol (1985) 2009; 106:1367-73. [PMID: 19036895].

35. Hulmi JJ, Silvennoinen M, Lehti M, Kivelä R, Kainulainen H. Altered REDD1, myostatin, and Akt/mTOR/FoxO/MAPK signaling in streptozotocin-induced diabetic muscle atrophy. Am J Physiol Endocrinol Metab 2012; 302:E307-15. [PMID: 22068602].

36. Saint-Martin Willer A, Santos-Gomes J, Adão R, Brás-Silva C, Eyries M, Pérez-Vizcaino F, Capuano V, Montani D, Antigny F. Physiological and pathophysiological roles of the KCNK3 potassium channel in the pulmonary circulation and the heart. J Physiol 2023; 601:3717-37. [PMID: 37477289].

37. Lescroart F, Kelly RG, Le Garrec J-F, Nicolas J-F, Meilhac SM, Buckingham M. Clonal analysis reveals common lineage relationships between head muscles and second heart field derivatives in the mouse embryo. Development 2010; 137:3269-79. [PMID: 20823066].

38. Pedrosa-Domellöf F, Eriksson PO, Butler-Browne GS, Thornell LE. Expression of alpha-cardiac myosin heavy chain in mammalian skeletal muscle. Experientia 1992; 48:491-4. [PMID: 1601115].

39. Bicer S, Reiser PJ. Complex tropomyosin and troponin T isoform expression patterns in orbital and global fibers of

adult dog and rat extraocular muscles. J Muscle Res Cell Motil 2013; 34:211-31. [PMID: 23700265].

40. Cerqua C, Morbidoni V, Desbats MA, Doimo M, Frasson C, Sacconi S, Baldoin MC, Sartori G, Basso G, Salviati L, Trevisson E. COX16 is required for assembly of cytochrome c oxidase in human cells and is involved in copper delivery to COX2. Biochim Biophys Acta Bioenerg 2018; 1859:244-52. [PMID: 29355485].

41. Morris SR, Gittings W, Vandenboom R. Epinephrine augments posttetanic potentiation in mouse skeletal muscle with and without myosin phosphorylation. Physiol Rep 2018; 6:e13690[PMID: 29718592].

42. Cairns SP, Borrani F. β-Adrenergic modulation of skeletal muscle contraction: key role of excitation-contraction coupling. J Physiol 2015; 593:4713-27. [PMID: 26400207].

43. De Paepe B, Zschüntzsch J, Šokčević T, Weis J, Schmidt J, De Bleecker JL. Šokčević, Weis J, Schmidt J, De Bleecker JL. Induction of osmolyte pathways in skeletal muscle inflammation: Novel biomarkers for myositis. Front Neurol 2018; 9:846-[PMID: 30364257].

44. De Paepe B, Martin JJ, Herbelet S, Jimenez-Mallebrera C, Iglesias E, Jou C, Weis J, De Bleecker JL. Activation of osmolyte pathways in inflammatory myopathy and Duchenne muscular dystrophy points to osmoregulation as a contributing pathogenic mechanism. Lab Invest 2016; 96:872-84. [PMID: 27322952].

45. Ross EA, Devitt A, Johnson JR. Macrophages: The good, the bad, and the gluttony. Front Immunol 2021; 12:708186[PMID: 34456917].

46. Lang CH. Importance of the innate immune response in skeletal muscle to sepsis-induced alterations in protein balance. Shock 2023; 59:214-23. [PMID: 36730901].

47. Philips C, Terrie L, Muylle E, Van Ginderdeuren R, Vereecke E, Mombaerts I, Thorrez L. The immunoarchitecture of human extraocular muscles. Invest Ophthalmol Vis Sci 2023; 64:23-[PMID: 37975851].

Articles are provided courtesy of Emory University and The Abraham J. & Phyllis Katz Foundation. The print version of this article was created on 30 September 2026. This reflects all typographical corrections and errata to the article through that date. Details of any changes may be found in the online version of the article.